The EMBO Journal vol.15 no.24 pp.7178–7187, 1996

Binding and kinetic properties of HIV-1 reverse transcriptase markedly differ during initiation and elongation of reverse transcription

Jean-Marc Lanchy, Chantal Ehresmann, Stuart F.J.Le Grice[1], Bernard Ehresmann and Roland Marquet[2]

Unité Propre de Recherche No. 9002 du Centre National de la Recherche Scientifique, Institut de Biologie Moléculaire et Cellulaire, 15 rue René Descartes, 67084 Strasbourg cedex, France and [1]Division of Infectious Diseases, Case Western Reserve University School of Medicine, Cleveland, OH 44106, USA

[2]Corresponding author

We recently showed that primer $tRNA_3^{Lys}$, human immunodeficiency virus type 1 (HIV-1) RNA and HIV-1 reverse transcriptase (RT) form a specific complex of initiation of reverse transcription that can be functionally distinguished from the elongation complex, which can be obtained by substituting an 18mer oligodeoxyribonucleotide (ODN) for the natural primer (Isel *et al.*, 1996). Here, we compared the binding properties and the single and multiple turnover kinetics of HIV-1 RT in the initiation and elongation complexes. Even though the equilibrium dissociation constants of HIV-1 RT are not very different for the two complexes, RT dissociates ~200-fold faster from the initiation complex. Furthermore, nucleotide incorporation by the preformed primer–template–RT complexes is reduced by a ~50-fold factor during initiation of reverse transcription, compared with elongation. As a consequence, processivity of HIV-1 RT in the initiation complex is close to unity, while it increases by four orders of magnitude during elongation, as expected for a replication enzyme. This processivity change is reminiscent of the transition from initiation to elongation of transcription. Furthermore, our results indicate that the post-transcriptional modifications of $tRNA_3^{Lys}$ play a role similar to that of the σ factor in transcription by the *Escherichia coli* RNA polymerase: they favour the formation of the specific initiation complex but do not affect the polymerization rate of the bound enzyme.

Keywords: HIV-1/kinetics/polymerase/replication/retrovirus

Introduction

Reverse transcriptase (RT) is a key enzyme of the retroviral cycle that converts the single-stranded RNA genome into double-stranded DNA (Baltimore, 1970; Temin and Mizutani, 1970). In retroviruses and retrotransposons, reverse transcription is a complex process that requires a multifunctional enzyme, which possesses RNA- and DNA-dependent DNA polymerase and RNase H activities, and also directs strand transfers (Gilboa *et al.*, 1979). Initiation of reverse transcription is primed by a tRNA whose 3′ end is complementary to the so called 'primer binding site' (PBS) (for a review see Marquet *et al.*, 1995). In addition to this 'general' PBS–tRNA interaction, evidence has recently accumulated for virus-specific interactions between the primer tRNA and the genomic RNA of avian retroviruses (Aiyar *et al.*, 1992, 1994), human immunodeficiency virus type 1 (HIV-1) (Isel *et al.*, 1993, 1995) and the yeast retrotransposon Ty1 (Wilhelm *et al.*, 1994; Friant *et al.*, 1996). These virus-specific interactions are required for efficient replication (Aiyar *et al.*, 1992; Wilhelm *et al.*, 1994; Wakefield *et al.*, 1996), suggesting that they are directly involved in the initiation of reverse transcription of retroviruses and retrotransposons.

In addition, initiation of DNA synthesis by the RTs encoded by hepadnaviruses (Wang and Seeger, 1992), mitochondrial plasmids (Wang and Lambowitz, 1993), group II introns (Zimmerly *et al.*, 1995) and bacteria (Shimamoto *et al.*, 1993) probably also relies on specific interactions. However, no detailed study of the kinetics of initiation of reverse transcription of any of these retroids was available so far. Indeed, detailed mechanistic characterization of the initiation and elongation stages of polymerases was achieved only in the case of RNA polymerases from bacteria and phages (von Hippel *et al.*, 1984; McClure, 1985). In these cases, initiation of transcription requires specific binding to a promoter and transition from a 'closed' to an 'open' complex. The initiation complex is capable of reiterative abortive initiation while remaining bound to the promoter. In *Escherichia coli*, transition from initiation to elongation is characterized by dissociation of the σ factor, conformational changes and translocation of the RNA polymerase, and is accompanied by dramatic changes in the kinetic parameters of the enzyme (von Hippel *et al.*, 1984; McClure, 1985).

In the case of retroviral reverse transcription, initiation has been recognized as a distinct and well-defined step of the replication process only very recently (Isel *et al.*, 1996). Indeed, we showed that primer $tRNA_3^{Lys}$, HIV-1 RNA and HIV-1 RT form a specific initiation complex that can be functionally distinguished from the elongation complex (Isel *et al.*, 1996). For example, elongation of HIV-1 reverse transcription is inhibited by manganese ions, while initiation is not. In HIV-1, transition from initiation to elongation takes place after extension by three to five nucleotides and is facilitated by an interaction between the anticodon of the primer tRNA and a viral A-rich loop located upstream of the PBS. When an 18mer oligodeoxyribonucleotide (ODN) complementary to the PBS is used as primer instead of $tRNA_3^{Lys}$, DNA synthesis starts in the elongation mode, without formation of an initiation complex (Isel *et al.*, 1996).

Whether the initiation and elongation steps of reverse transcription differ by their binding and/or catalytic properties (and to what extent) remained unanswered. This study

is the first quantitative comparison of the initiation and elongation steps of reverse transcription. It turns out that both the binding and kinetic properties of HIV-1 RT differ markedly during initiation and elongation. We found that, as previously observed for transcription by bacterial and viral RNA polymerases, initiation is a slow process compared with elongation and proceeds with a highly reduced processivity. Moreover, the post-transcriptional modifications of $tRNA_3^{Lys}$ favour the formation of a productive initiation complex, but do not affect its polymerization rate.

Results

Since the rate of nucleotide addition by HIV-1 RT may be sequence dependent, we did not study initiation and elongation of reverse transcription by following the sequential extension of $tRNA_3^{Lys}$ through these two polymerization modes. Rather, we used the $tRNA_3^{Lys}$–viral RNA–RT and ODN–viral RNA–RT complexes to compare nucleotide incorporation in the initiation and elongation modes using the same template sequence. The template was an *in vitro* synthesized RNA corresponding to nucleotides 1–311 of HIV-1 genomic RNA, which contains the PBS (nucleotides 179–196). As a control, we formed a non-specific initiation complex by using a synthetic version of human $tRNA_3^{Lys}$ lacking all post-transcriptional modifications ($utRNA_3^{Lys}$) as primer. Indeed, we showed previously that the post-transcriptional modifications of $tRNA_3^{Lys}$ are a major determinant of the specificity of the binary primer–template complex (Isel *et al.*, 1993, 1995) and of the ternary primer–template–RT complex (Isel *et al.*, 1996).

We studied the multiple and single turnover kinetics of addition of one or two nucleotides to ODN, $tRNA_3^{Lys}$ and $utRNA_3^{Lys}$, as well as the binding parameters of HIV-1 RT to the corresponding primer–templates. Addition of two consecutive nucleotides was used to allow a more precise quantification when using $tRNA_3^{Lys}$ and $utRNA_3^{Lys}$ as primers. This was justified by the fact that HIV-1 RT did not dissociate at +1 position in any of the complexes studied here (Isel *et al.*, 1996) and that no (ODN primer) or almost no (other primers) +1 product was detected in the multiple and single turnover kinetics, indicating that addition of the second nucleotide was not the rate-limiting step.

Steady state kinetics

First, we looked at multiple turnover kinetics by using a large excess of primer–template compared with RT. When 100 nM of primer–template were extended with 3 nM of HIV-1 RT, the amount of extended products increased linearly over time, as expected for a steady-state process (Figure 1). While extension of ODN and $utRNA_3^{Lys}$ occurred at similar rates, extension of $tRNA_3^{Lys}$ was 32- to 35-fold faster. The slopes of the straight lines of Figure 1A, which are directly proportional to the rate constant of addition of the two nucleotides (k_{cat}), are 0.0048, 0.0053 and 0.170 nM/s for $utRNA_3^{Lys}$, ODN and $tRNA_3^{Lys}$, respectively. The rate constant k_{cat} is obtained for each primer by dividing the slope by the concentration of active enzyme. A lower estimate of the fraction of active RT is 40% (see below). Thus, the k_{cat} for nucleotide addition to

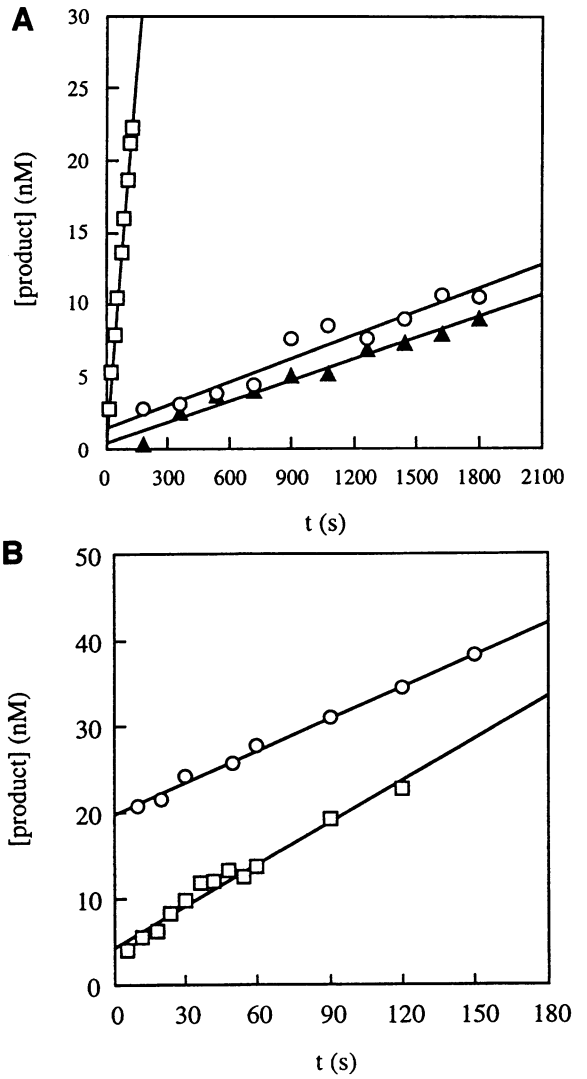

Fig. 1. Steady-state kinetics. (**A**) Primer–templates (100 nM) were incubated with 3 nM HIV-1 RT for 4 min and reaction was initiated by addition of 50 μM dCTP and ddTTP. The primer was $tRNA_3^{Lys}$ (□), $utRNA_3^{Lys}$ (▲) or ODN (○). (**B**) ODN–viral RNA (150 nM) (○) and $tRNA_3^{Lys}$–viral RNA (100 nM) (□) were incubated with 50 and 10 nM RT, respectively.

$utRNA_3^{Lys}$, ODN and $tRNA_3^{Lys}$, determined from three to six independent experiments, is 0.0042 ± 0.0003, 0.0031 ± 0.0008 and 0.11 ± 0.05/s, respectively (Table I). When using $tRNA_3^{Lys}$ or $utRNA_3^{Lys}$, similar k_{cat} values were obtained using either the wild type HIV-1 RT or the RNase H(–) mutant enzyme (data not shown). These rate constants correspond to the overall reaction:

$$P/T + RT \xrightarrow{k_{cat}} (P + 2)/T + RT$$

where P/T is the primer–template complex and (P+2) is the primer extended by two nucleotides.

From the data of Figure 1A, it is difficult to evaluate precisely whether the lines extrapolate through the origin of the graph. Using ODN and $tRNA_3^{Lys}$ as primers, we performed additional experiments in which the (primer–template):RT ratio was adjusted for each primer to obtain similar rates of product formation and the reaction time was reduced to remain in the steady-state phase (Figure

Table I. Binding and kinetic properties of HIV-1 RT during initiation and elongation of reverse transcription

Polymerization mode	Elongation	Initiation	Non-specific initiation
Primer	ODN	$tRNA_3^{Lys}$	$utRNA_3^{Lys}$
K_d (nM)	1.0 ± 0.1	2.7 ± 0.4	non-specific binding
k_{off}^0 (s^{-1})	0.0010 ± 0.0001	0.21 ± 0.03	n.d.[a]
k_{cat} (s^{-1})	0.0031 ± 0.0008	0.11 ± 0.05	0.0042 ± 0.0003
k_{on}^0 (μM^{-1} s^{-1})[b]	1	77	n.d.
k_{pol} (s^{-1})	13 ± 3	0.22 ± 0.03	0.18 ± 0.06
Processivity[c]	13 000	1	<<1[d]

All data are from three to six independent experiments.
[a]n.d., not determined.
[b]$k_{on}^0 = k_{off}^0/K_d$.
[c]Processivity = k_{pol}/k_{off}^0.
[d]From elongation with trap.

1B). Under these conditions, the existence of a burst during extension of ODN and $tRNA_3^{Lys}$ by HIV-1 RT is clearly apparent. The intercept at the origin indicates that extension of the ODN–viral RNA–RT and $tRNA_3^{Lys}$–viral RNA–RT complexes formed during pre-incubation is faster than during the following turnovers. Thus, the rate-limiting step during steady-state extension of ODN and $tRNA_3^{Lys}$ follows the catalytic step.

In both cases the rate-limiting step is most probably dissociation of RT from the primer–template complex after nucleotide addition. This result was confirmed by directly measuring the dissociation rate of RT from the ODN–viral RNA and $tRNA_3^{Lys}$–viral RNA complexes (see below). In the case of $tRNA_3^{Lys}$, we further eliminated the possibility that the limiting event was binding of RT to the primer–template complex by performing steady state kinetics at a constant RT concentration (3 nM) while increasing the $tRNA_3^{Lys}$–viral RNA concentration from 10 to 100 nM. Contrary to what would be observed if formation of the ternary complex was rate limiting, k_{cat} is independent of the primer–template concentration (data not shown).

Since dissociation of RT from the ODN–viral RNA and $tRNA_3^{Lys}$–viral RNA complexes extended by two nucleotides is rate-limiting, the k_{cat} values correspond to the rate constants for RT dissociation at position +2 (k_{off}^{+2}) of ODN and $tRNA_3^{Lys}$. Thus, the lifetime of the (ODN+2)–viral RNA–RT and ($tRNA_3^{Lys}$+2)–viral RNA–RT complexes equals $1/k_{cat}$, i.e. ~5 min and 9 s respectively.

When using short primer–templates, the amplitude of the burst can be used to evaluate the fraction of active enzyme (Kati *et al.*, 1992; Hsieh *et al.*, 1993). However, in this study we used a long RNA template to which RT also binds in a non-specific manner and the amplitude of the burst rather gives a lower limit of the fraction of active RT. From Figure 1B, one can conclude that ~40% (20 nM/50 nM with ODN, and 4 nM/10 nM with $tRNA_3^{Lys}$) of RT was initially bound to the ODN–viral RNA complex in a 'productive' manner. We used this lower estimate of the fraction of active enzyme to determine the k_{cat} values (see above).

Single turnover kinetics

The rate constant (k_{pol}) for primer extension by the pre-formed primer–template–RT complex (P/T·RT) which corresponds to:

$$\text{P/T·RT} \xrightarrow{k_{pol}} \text{(P + 1)/T·RT}$$

can be determined by decreasing the (primer–template):RT ratio. Under these conditions, we were looking at nucleotide incorporation during a single enzymatic cycle.

Incorporation of one nucleotide in the pre-formed ODN–viral RNA–RT is very fast (Figure 2A). The amplitude of the burst, i.e. the amount of product formed during a single enzymatic cycle, slightly increases when the RT to ODN–viral RNA ratio increases from 2 to 40, indicating that the enzyme is not totally bound to the primer–template at a 2:1 ratio. However, the rate constant for nucleotide incorporation (k_{pol}) is almost independent of the RT to ODN–viral RNA ratio. Multiple experiments yield k_{pol} of 10 ± 1 and 13 ± 3 s^{-1} at 2- and 40-fold excess of RT relative to the primer–template respectively (Figure 2A and Table I). This is expected because nucleotide incorporation is much faster than dissociation of RT from the primer–template (see above). A similar result was observed when using oligodeoxyribonucleotides as primers and short RNA or DNA oligomers as templates (Kati *et al.*, 1992; Reardon, 1992; Hsieh *et al.*, 1993). Since k_{pol} does not take binding and dissociation of RT from the primer–template into account, it reflects the polymerization rate under conditions of processive synthesis. Thus, in the presence of the four dNTPs ~13 nucleotides would be incorporated per second in the elongation complex.

Surprisingly, nucleotide incorporation was much slower in the initiation complex than in the elongation one (Figure 2B). In this case, the data require a sum of two first-order processes to be correctly fitted. The amplitude of the fast one increases with the RT to $tRNA_3^{Lys}$–viral RNA ratio, and saturates at 55–60% of $tRNA_3^{Lys}$ extension at high RT excess (Figure 2B). In contrast with our results with ODN, the corresponding apparent extension rate constant (k_{pol}^{app}) of $tRNA_3^{Lys}$ strongly depends on the RT concentration (Figure 2B). This is expected when polymerization occurs at a similar rate to enzyme dissociation. In this case, addition of one single nucleotide may require several binding events. Thus, at low enzyme concentration k_{pol}^{app} does not only reflect the polymerization rate (k_{pol}), but also the binding rate of RT to the primer–template (k_{on}). Thus, a correct approximation of k_{pol} can only be obtained at high RT concentration, when binding of RT is much faster than polymerization. A systematic study of the dependence of k_{pol}^{app} on the RT concentration shows that

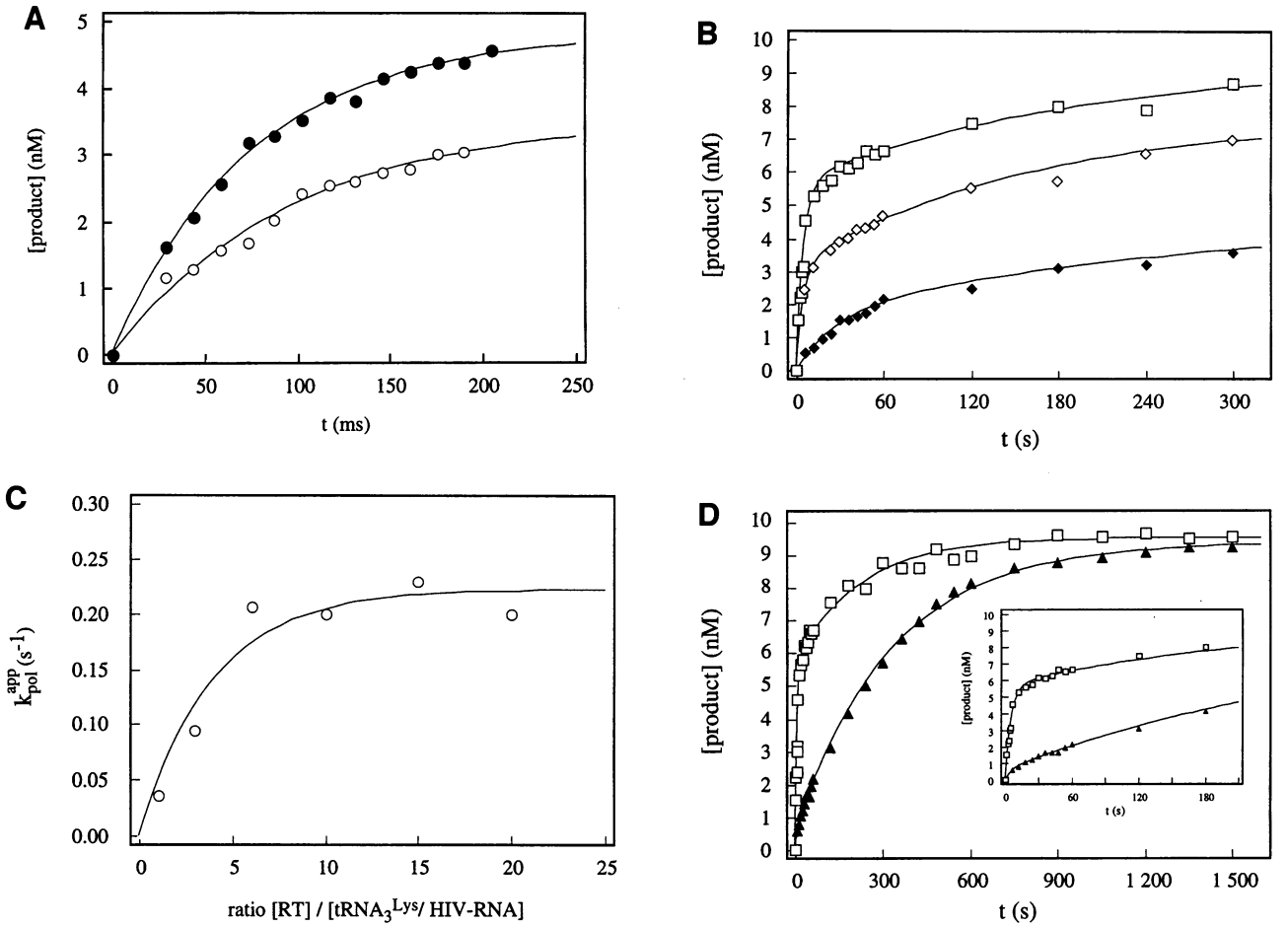

Fig. 2. Single turnover kinetics. (**A**) Five nM of ODN–viral RNA were incubated with 10 nM (○) or 200 nM (●) of HIV-1 RT (not corrected for the fraction of active enzyme) and reaction was initiated by addition of 50 μM dCTP. Reaction was performed in home-build apparatus (see Materials and methods). Data in the burst phase were fitted according to:

$$[P + 1] = A \cdot (1-e^{-k_{pol} \cdot t})$$

where P + 1 is the primer extended by one nucleotide and A is the amplitude of the burst. The best fits were obtained with A = 3.45 nM and k_{pol} = 10 s^{-1}, at 10 nM RT, and A = 4.85 nM and k_{pol} = 13 s^{-1}, at 200 nM RT. (**B**) Ten nM of $tRNA_3^{Lys}$–viral RNA were incubated with 10 (◆), 100 (◇) or 200 (□) nM of HIV-1 RT and reactions were initiated by addition of 50 μM dCTP and ddTTP. Data were fitted using the relationship:

$$[P + 2] = A \cdot (1-e^{-k_{pol}^{app} \cdot t}) + B \cdot (1-e^{-k_{slow} \cdot t})$$

where A and B represent the amplitude of the fast and the slow processes respectively, k_{pol}^{app} is the apparent extension rate constant, and k_{slow} is the rate constant of the slow process. The best fits were obtained with: A = 1.7 nM, k_{pol}^{app} = 0.036 s^{-1}, B = 3.3 nM, k_{slow} = 0.003 s^{-1} at 10 nM RT; A = 3.2 nM, k_{pol}^{app} = 0.20 s^{-1}, B = 4.5 nM, k_{slow} = 0.006 s^{-1} at 100 nM RT; and A = 5.7 nM, k_{pol}^{app} = 0.20 s^{-1}, B = 3.7 nM, k_{slow} = 0.005 s^{-1} at 200 nM RT. (**C**) Dependence of the apparent extension rate constant (k_{pol}^{app}) on the RT to $tRNA_3^{Lys}$–viral RNA ratio. The concentration of the primer–template complex was kept constant (10 nM). Fitting of the relationship:

$$k^{app}{}_{pol} = k_{pol} \cdot (1-e^{-K \cdot \{[RT]/[P/T]\}})$$

to the experimental data yielded k_{pol} = 0.22 s^{-1}. (**D**) Ten nM of $tRNA_3^{Lys}$–viral RNA (□) or $utRNA_3^{Lys}$–viral RNA (▲) were incubated with 200 nM of HIV-1 RT and reactions were initiated by addition of 50 μM dCTP and ddTTP. Data were analysed as in (B). The best fit for the $utRNA_3^{Lys}$–viral RNA primer–template was obtained with A = 0.6 nM, k_{pol}^{app} = 0.18 s^{-1}, B = 8.7 nM, k_{slow} = 0.003 s^{-1}. The inset is an enlargement of the data collected within the first 3 min of reaction that allows a better visualisation of the fast process and transition to the slow one.

the k_{pol} value for nucleotide incorporation is equal to 0.22 ± 0.03 s^{-1} (Figure 2C and Table I), indicating that statistically the initiation complex performs only one catalytic event every 4–5 s. The k_{pol} value determined for $tRNA_3^{Lys}$ (and $utRNA_3^{Lys}$) corresponds to addition of two nucleotides. However, polyacrylamide gel analysis shows that the concentration of the transient +1 product is low, indicating that addition of the second nucleotide is faster than that of the first one (data not shown). Thus, k_{pol} mainly reflects addition of the first nucleotide.

The rate constant of the slow process (k_{slow}) observed during extension of $tRNA_3^{Lys}$ is 0.005 ± 0.002 s^{-1}, i.e. ~20-fold lower than k_{cat} (Figure 2B). No dependence of k_{slow} on the RT concentration was observed (Figure 2B and data not shown). The fact that extension of $tRNA_3^{Lys}$ is biphasic can be explained by two different models. In the first one, the $tRNA_3^{Lys}$–viral RNA complex would exist under two conformations, and only one of them would allow productive binding of RT. In the second, the primer–template would assume a single conformation but two alternative $tRNA_3^{Lys}$–viral RNA–RT ternary complexes could be formed: a 'productive' one and an 'unproductive one'. In the first model, the slow process would correspond to the transition of the 'unproductive' con-

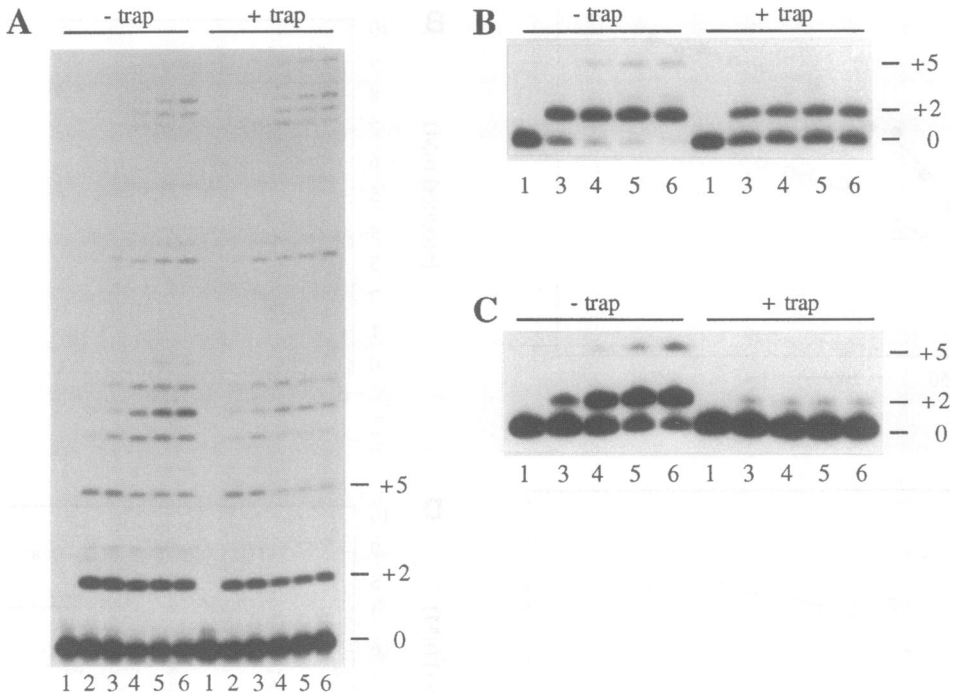

Fig. 3. Extension of 20 nM ODN (**A**), $tRNA_3^{Lys}$ (**B**) and $utRNA_3^{Lys}$ (**C**) by 20 nM RT in the presence of poly(rA)·$(dT)_{15}$. Primer–templates were incubated at 37°C for 4 min and reactions were initiated by addition of dCTP and dTTP (50 μM each) in the absence or presence of excess poly(rA)·$(dT)_{15}$. Lanes 1 to 6 correspond to reaction for 0, 30 s, 1, 5, 10 and 15 min, respectively.

formation of the primer–template into the 'productive' one. In the second, k_{slow} would reflect the conversion of the unproductive ternary complex into a productive one. Indeed, one can easily discriminate between these two models on the basis of the steady-state data obtained in the presence of a large excess of primer–template. According to the first model, the productive conformer of the primer–template would also be in excess compared with RT, and the conformational change in the binary complex would not be detected. If the second model holds, unproductive ternary complex would be formed independently of the primer–template concentration, and its conversion into productive ternary complex would be rate limiting in steady-state kinetics. Since k_{cat} is 20-fold greater than k_{slow}, the second model can be ruled out. Thus, the two first-order processes that we used to fit the data correspond to:

$$(P/T)^{prod} \cdot RT \xrightarrow{k_{pol}} (P + 1)/T \cdot RT \quad (fast)$$

$$(P/T)^{unprod} \xrightarrow{k_{slow}} (P/T)^{prod} \quad (slow)$$

where the superscripts 'prod' and 'unprod' stand for productive and unproductive, respectively.

Extension of $utRNA_3^{Lys}$ was much slower than that of $tRNA_3^{Lys}$, even when using a 20-fold excess of RT over primer–template (Figure 2D). Nevertheless, extension of $utRNA_3^{Lys}$ is also fitted correctly by the sum of two first-order processes. Interestingly, in the presence of a large excess of RT, the k_{pol}^{app} ($0.18 \pm 0.06\ s^{-1}$) and k_{slow} (0.003 ± 0.001) values are the same, within the experimental errors, as those measured for extension of the natural tRNA. The slower extension of $utRNA_3^{Lys}$ is due to a very low contribution of the fast step to the overall process, as clearly shown in the insert of Figure 2D. These results suggest that the absence of the post-transcriptional modifications of $tRNA_3^{Lys}$ does not affect the polymerization step itself but strongly influences the fraction of primer–template that can productively sustain extension.

Binding constant of RT to the primer–template

Determination of the equilibrium binding constant of RT to various primer–template complexes and measurement of the dissociation rate of RT from these complexes requires distinguishing between bound and free enzyme. This distinction is possible by using a trap that binds to the free enzyme, while allowing primer extension by the bound enzyme (Beard and Wilson, 1993; DeStefano *et al.*, 1993; Hsieh *et al.*, 1993; Jaju *et al.*, 1995). However, this methodology requires that extension of the primer by the bound enzyme is faster than enzyme dissociation, or at least of the same order of magnitude. Therefore, we first checked whether primer extension was observed when the trap was added, together with dCTP and dTTP, to the preformed primer–template–RT complexes.

Efficient extension of ODN was observed in the presence of the trap (Figure 3A), in agreement with the corresponding value of k_{pol} and the fact that dissociation of HIV-1 RT from ODN–RNA hybrids is slow (see steady-state experiments for dissociation at position +2, and below for dissociation from the ODN–viral RNA before nucleotide incorporation). Indeed, even though only dCTP and dTTP were included in the reaction mixture, up to 20 nucleotides were incorporated in the presence of the trap, indicating that nucleotide misincorporation and extension of the mismatches were also faster than dissociation of RT.

Significant extension of $tRNA_3^{Lys}$ was also observed in the presence of an excess of poly(rA)·$(dT)_{15}$ (Figure

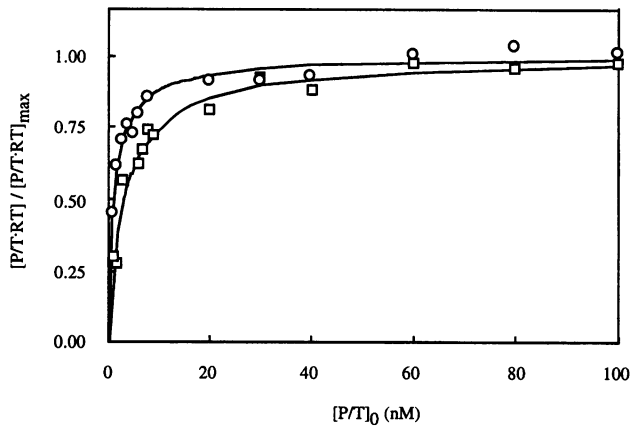

Fig. 4. Dissociation constant of the primer–template–RT complexes. Increasing concentrations of primer–template ($[P/T]_0$) were equilibrated with equimolar amounts of RT (not corrected for the fraction of active enzyme) at 37°C for 4 min and the amount of primer–template–RT (P/T-RT) at equilibrium was determined by addition of nucleotides and poly(rA)·$(dT)_{15}$ (see Materials and methods). Fitting of the data according to:

$$\frac{[P/T\cdot RT]}{[P/T]_0} = \frac{K_d + 2[P/T]_0 - \sqrt{(K_d + 2[P/T]_0)^2 - 4[P/T]_0^2}}{2[P/T]_0}$$

yields K_d values of 1.0 and 2.7 nM when using ODN (○) and $tRNA_3^{Lys}$ (□) as primer, respectively.

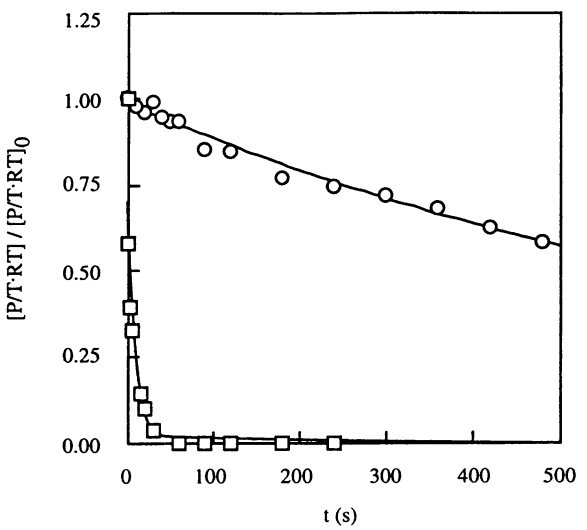

Fig. 5. Kinetics of dissociation of the primer–template–RT complexes. Ten nM of ODN–viral RNA (○) or $tRNA_3^{Lys}$–viral RNA (□) were pre-incubated with 50 nM of RT for 4 min at 37°C, and dissociation of RT from the primer–templates was measured as described in Materials and methods. Fitting of the experimental data to the equation:

$$\frac{[P/T\cdot RT]}{[P/T\cdot RT]_0} = e^{-k_{off}\cdot t}$$

yields k_{off} values of 0.0010 and 0.21 s^{-1}, respectively.

3B). However, no misincorporation was detected during extension of the natural primer in the presence of the trap. In the absence of the trap, only a faint band corresponding to the +5 product was detected, indicating very low misincorporation. As could be expected from the results of Figure 2D, almost no extension of $utRNA_3^{Lys}$ was detected in the presence of poly(rA)·$(dT)_{15}$ (Figure 3C). Indeed, no significant extension of $utRNA_3^{Lys}$ could be observed in the presence of the trap, even when using increasing excess (up to 20-fold) of RT over primer–template, while a maximum of ~50% of $tRNA_3^{Lys}$ was extended under these conditions (data not shown).

Direct evaluation of the K_d of RT for ODN–viral RNA and $tRNA_3^{Lys}$–viral RNA corresponding to the equilibrium:

$$P/T + RT \underset{}{\overset{K_d}{\longleftrightarrow}} P/T\cdot RT$$

was determined by extending increasing concentrations of primer–template by stoichiometric amounts of RT in the presence of a trap, as described in Materials and methods (Figure 4). The affinity of RT is only slightly better for ODN–viral RNA (K_d = 1.0 ± 0.1 nM) than for $tRNA_3^{Lys}$–viral RNA (K_d = 2.7 ± 0.4 nM).

Due to the absence of nucleotide incorporation in the presence of the trap, the affinity of HIV-1 RT for $utRNA_3^{Lys}$–viral RNA could not be evaluated directly. Thus, we looked for an inhibitory effect of increasing amounts of $utRNA_3^{Lys}$–viral RNA on nucleotide incorporation in ODN–viral RNA and $tRNA_3^{Lys}$–viral RNA complexes. In fact, we were unable to detect any difference between the $utRNA_3^{Lys}$–viral RNA and the viral RNA alone in their inhibitory effect on ODN and $tRNA_3^{Lys}$ extension (data not shown). We conclude that $utRNA_3^{Lys}$ is not specifically recognized as a primer by HIV-1 RT and that there is no preferential binding of RT to the PBS of the $utRNA_3^{Lys}$–viral RNA complex.

Dissociation rate constant of the primer–template–RT complex

By using poly(rA).$(dT)_{15}$ to trap the free enzyme, it was also possible to measure directly the dissociation of the enzyme from ODN–viral RNA and $tRNA_3^{Lys}$–viral RNA, before catalysis:

$$P/T\cdot RT \xrightarrow{k_{off}^0} P/T + RT$$

A dramatic difference was observed between initiation and elongation complexes (Figure 5). Dissociation of HIV-1 RT from the elongation complex was slow: the measured k_{off}^0 (0.0010 ± 0.0001 s^{-1}) corresponds to a mean lifetime of the elongation complex of ~17 min. In contrast, HIV-1 RT completely dissociates from the initiation complex in <20 s, and the mean lifetime of the initiation complex is ~5 s (Figure 5 and Table I).

Discussion

We recently showed that initiation and elongation of HIV-1 reverse transcription are two different steps that can be distinguished functionally (Isel *et al.*, 1996). Specific initiation of reverse transcription was observed with the homologous $tRNA_3^{Lys}$–HIV-1 genomic RNA–HIV-1 RT complex, while a synthetic version of the tRNA was a very poor primer. When reverse transcription was primed by ODN, no initiation complex was formed and DNA synthesis started in the elongation mode (Isel *et al.*, 1996). Here, we performed a comparative study of the binding and kinetic properties of HIV-1 RT in the initiation

and elongation complexes. As summarized in Table I, these properties differ dramatically in the two complexes.

As expected, the binding and kinetic properties of HIV-1 RT in the ODN–viral RNA–HIV-1 RT complex that we determined in this study are reminiscent of those previously obtained when using oligodeoxyribonucleotides as primers and short RNA or DNA oligomers as templates (Kati *et al.*, 1992; Reardon, 1992, 1993; Hsieh *et al.*, 1993). Indeed, RT is expected to form non-specific elongation complexes when binding to these primer–template models, just as it does with ODN–HIV-1 RNA (Isel *et al.*, 1996). With these model systems, the rate limiting step during steady-state elongation of oligodeoxyribonucleotides is also dissociation of HIV-1 RT from the primer–template (Kati *et al.*, 1992; Reardon, 1992, 1993; Hsieh *et al.*, 1993). The first order rate constant for nucleotide incorporation (k_{pol}) that we measured with ODN–HIV-1 RNA ($13 \pm 3\ s^{-1}$, Table I) is in the range of that measured by others using oligoribonucleotides as templates (Kati *et al.*, 1992; Reardon, 1992, 1993). Thus, nucleotide incorporation by HIV-1 RT during elongation complex is rather fast, as expected for a replicative enzyme that has to reverse transcribe ~10 kb.

The steady-state k_{cat} values, and thus the dissociation rates from the extended primers, obtained with the oligodeoxyribonucleotide–oligoribonucleotide primer–templates (0.06–0.08 s^{-1}) (Kati *et al.*, 1992; Reardon, 1993), are more than one order of magnitude higher than the k_{cat} determined here for the ODN–viral RNA complex (Table I). When measuring directly k_{off}^0, the difference between model primer–templates and our complex using a large natural template is even more pronounced: HIV-1 RT dissociates 75- to 180-fold faster from short templates (Kati *et al.*, 1992; Reardon, 1993) than from the 311-nucleotide fragment of HIV-1 genomic RNA (Table I). These data suggest that a long template strengthens binding of HIV-1 RT to DNA–RNA hybrids. The more pronounced effect of the template length on k_{off}^0 compared with k_{cat} may be due to the fact the determination of k_{off}^0 with short templates was conducted in the absence of magnesium (DeStefano *et al.*, 1993). Similarly, using the 18mer ODN as primer, the K_d of HIV-1 RT decreases from 38 to 5 nM when the length of the DNA template increases from 19 to 31 nucleotides (Patel *et al.*, 1995). Thus, it appears that the dependence of the RT binding on the template length is probably a general phenomenon.

On the contrary, RT binds 4- to 8-fold faster when using a short RNA template (Kati *et al.*, 1992; Reardon, 1993) than with our long HIV-1 RNA (Table I). The slower binding to the longer template may reflect either a one-dimensional search of the primer along the template, or occurrence of non-specific binding and dissociation events before binding to the annealed primer. In keeping with the stronger influence of the template length on k_{off} compared with k_{on}, the K_d value that we determined for the ODN–viral RNA–RT complex (1.0 nM, Table I) is significantly lower than that previously measured by others using short DNA–RNA hybrids (5–10 nM) (Kati *et al.*, 1992; Reardon, 1992, 1993).

Our analysis of the kinetic and binding properties of HIV-1 RT in the initiation complex is the first quantitative study of the initiation of reverse transcription. It reveals clear differences between initiation and elongation of reverse transcription concerning binding of HIV-1 RT to these complexes and the rate of nucleotide incorporation (Table I). Even though the K_ds of RT binding to ODN–viral RNA and $tRNA_3^{Lys}$–HIV-1 RNA differ only by 2.7-fold, they result from very different binding and dissociation rates (Table I). HIV-1 RT dissociates ~200-fold faster from the initiation complex than from the elongation complex. As a replicative enzyme, HIV-1 RT must achieve processive synthesis using either DNA–RNA or DNA–DNA primer–templates, while the use of an RNA–RNA hybrid is an exception that occurs only during initiation of reverse transcription. Therefore, a strong selection pressure probably exists to select enzymes that dissociate slowly from the elongation complex. At the opposite, HIV-1 RT binds ~80-fold faster to $tRNA_3^{Lys}$–HIV-1 RNA than to ODN–viral RNA. In the case of the elongation complex, the primer–template binds in a large cleft formed by the fingers, palm and thumb of the p66 subunit of HIV-1 RT (Arnold *et al.*, 1992; Kohlstaedt *et al.*, 1992; Jacobo-Molina *et al.*, 1993). In contrast, it is not only the 3′ end that is annealed to the PBS, but other regions of $tRNA_3^{Lys}$ and its post-transcriptional modifications are involved in formation of the initiation complex (Isel *et al.*, 1996). Interactions with these regions and post-transcriptional modifications of $tRNA_3^{Lys}$ may anchor HIV-1 RT on the $tRNA_3^{Lys}$–HIV-1 RNA complex and hasten subsequent binding of the primer–template in the cleft of the p66 subunit. This hypothesis is supported by the fact that we were unable to detect any specific binding of HIV RT to $utRNA_3^{Lys}$–HIV-1 RNA.

More unexpected than the differences in binding properties of HIV-1 RT is the difference in the polymerization rate during initiation and elongation of reverse transcription. Indeed, nucleotide addition by the initiation complex is two orders of magnitude slower than by the elongation complex (Table I). This extremely low rate of nucleotide incorporation during initiation of reverse transcription is comparable to the rate of nucleotide addition by the elongation complex in the presence of saturating amounts of non-nucleoside inhibitors (Spence *et al.*, 1995). The very slow rate of nucleotide addition during initiation compared with elongation of reverse transcription may seem contradictory to our previous finding that $tRNA_3^{Lys}$ was more efficiently extended than ODN during the course of (–) strong stop DNA synthesis (Isel *et al.*, 1996). Indeed, the latter study corresponded to multiple turnover kinetics, and the slow extension of ODN was due to slow dissociation of RT from the elongation complex, while fast recycling of the enzyme took place with $tRNA_3^{Lys}$ as primer (Isel *et al.*, 1996).

In contrast with what was observed for the elongation complex by us (this study with ODN as primer) and others (Kati *et al.*, 1992; Reardon, 1992), extension of natural and synthetic $tRNA_3^{Lys}$ appeared to be a biphasic process, even in the presence of large excess of RT. A maximum of 55–60% of $tRNA_3^{Lys}$ was extended in the fast reaction, and the remaining primer was extended very slowly. The most likely explanation is that the $tRNA_3^{Lys}$–viral RNA complexes exist under two conformations, and that only one of them allows productive binding of RT. The slow process probably corresponds to the transition from an 'unproductive' conformation of the primer–template into a 'productive' one. Interestingly, binding and kinetic data

indicate that specific binding of HIV-1 RT is lost when *utRNA$_3^{Lys}$* is substituted for the natural primer, but the rate of nucleotide addition (k_{pol}) is not affected (Table I). This result is in keeping with the fact that the same RNA–RNA hybrid is bound in the cleft containing the polymerization site of HIV-1 RT when using either natural or synthetic tRNA$_3^{Lys}$.

It was clearly shown that the rate-limiting step during addition of a single nucleotide in the pre-formed elongation complex is not the chemical step itself. Instead, the k_{pol} value reflects a rate limiting conformational change of RT preceding the chemical step (Kati *et al.*, 1992; Hsieh *et al.*, 1993; Reardon, 1993; Rittinger *et al.*, 1995). The rate-limiting step during nucleotide addition in the initiation complex is probably also a conformational change of HIV-1 RT, since (i) incorporation of αS-dCMP is as fast as incorporation of dCMP, and (ii) substitution of Mn^{2+} for Mg^{2+} does not affect the k_{pol} value (J.M.Lanchy, unpublished data). If the chemical step were rate limiting, a strong decrease in k_{pol} for incorporation of αS-dCMP should be observed (Wong *et al.*, 1981), and since bivalent cations are directly involved in phosphodiester bond formation (Patel *et al.*, 1995), k_{pol} should be strongly affected when substituting Mn^{2+} for Mg^{2+}.

Thus, the rate-limiting step of nucleotide addition is most likely a conformational change of RT in both the initiation and elongation stage of reverse transcription. Consequently, this conformational change should be 50-fold faster in the elongation mode than in the initiation mode. On the other hand, the conformation of RT required for the phosphodiester bond formation is probably the same in the two polymerization modes. Therefore, our results suggest that RT initially binds in different conformations to the initiation and elongation complexes, in agreement with our previous finding (Isel *et al.*, 1996).

As a consequence of the differences in dissociation and polymerization rates, processivity of polymerization is four orders of magnitude lower during initiation than during elongation of reverse transcription (Table I). If elongation was unaffected by the primary and secondary structures of the template, HIV-1 RT would reverse transcribe ~10 kb before dissociating from the elongation complex. This value is significantly higher than the 340 value determined for DNA synthesis using short RNA templates (Reardon, 1993). As explained above, this difference reflects faster dissociation of HIV-1 RT when using short model templates. Our results indicate that under favourable conditions, HIV-1 RT displays a processivity similar to that of other replicative enzymes, such as T7 DNA polymerase (Patel *et al.*, 1991). However, several pausing sites are observed during (–) strong stop DNA synthesis (Isel *et al.*, 1996), indicating that processivity varies strongly along the template. Furthermore, processivity of HIV-1 RT is up to 70-fold higher when using RNA templates rather than their DNA counterparts (Reardon, 1993). In contrast to elongation, processivity during initiation is close to unity, indicating that dissociation of HIV-1 RT from the initiation complex is as probable as extension of tRNA$_3^{Lys}$ by one nucleotide.

The differences that we observed between initiation and elongation of reverse transcription present interesting analogies with RNA synthesis by the *E.coli* RNA polymerase holoenzyme (von Hippel *et al.*, 1984; McClure, 1985) or by RNA polymerases from phages (Martin *et al.*, 1988). Initiation of RNA synthesis by *E.coli* RNA polymerase is slow compared with elongation. Some limiting factors are specific for RNA polymerases, such as formation of an open complex (von Hippel *et al.*, 1984; McClure, 1985). However, abortive synthesis of short oligoribonucleotides and polymerase pausing near the start site (without dissociation) are frequently limiting factors of long chain RNA synthesis, indicating reduced processivity during initiation of transcription (von Hippel *et al.*, 1984; McClure, 1985). Reduced processivity was also observed in the early stages of transcription by T7 RNA polymerase. It was attributed to a reduced polymerization rate (by ~200-fold) and greater dissociation rate in initiation compared with elongation of transcription (Martin *et al.*, 1988). In *E.coli*, the regulatory subunit σ of the RNA polymerase is required for formation of the specific initiation complex (von Hippel *et al.*, 1984; McClure, 1985). Our present and previous (Isel *et al.*, 1996) data indicate that a similar functional role can be attributed to the post-transcriptional modifications of tRNA$_3^{Lys}$ in the initiation of HIV-1 reverse transcription.

Taken together, our results clearly show that the binding and kinetic properties of HIV-1 RT differ dramatically during initiation and elongation of reverse transcription. Due to the unique properties of HIV-1 RT during initiation, this step may represent a specific target for anti-HIV-1 compounds. For instance, the slow polymerization rate may render the initiation complex particularly sensitive to nucleotide analogues bearing reactive groups that could modify the polymerization active site of HIV-1 RT. Due to the specific interactions between the components of the initiation complex and the fact that one of them (tRNA$_3^{Lys}$) is not allowed to mutate, emergence of escape mutants may be limited in the presence of efficient inhibitors of initiation of reverse transcription.

Materials and methods

Template, primers and RTs

In all experiments, the template was an RNA corresponding to nucleotides 1–311 of HIV-1 genomic RNA (Mal isolate) that was synthesized by *in vitro* transcription with RNA polymerase from phage T7 as previously described (Marquet *et al.*, 1991). Natural tRNA$_3^{Lys}$ was purified either from beef liver or from chicken liver as described in Isel *et al.* (1993). Its sequence and post-transcriptional modifications are identical to those of human tRNA$_3^{Lys}$ (G.Keith, personal communication). Synthetic *utRNA$_3^{Lys}$* was obtained by *in vitro* transcription of the corresponding artificial gene inserted in pUC18 in the presence of 16 mM GMP to favour the synthesis of 5′ monophosphorylated products (Isel *et al.*, 1993). tRNA$_3^{Lys}$ and *utRNA$_3^{Lys}$* were 3′ end-labelled with [α-^{32}P]ATP (NEN) (Isel *et al.*, 1993). ODN was chemically synthesized and 5′ end-labelled with [γ-^{32}P]ATP (NEN) and polynucleotide kinase from phage T4 (USB) (Isel *et al.*, 1993). Template RNA was hybridized with ^{32}P-labelled primer at a 2:1 ratio as previously described (Isel *et al.*, 1993). The concentration of primer–template was corrected for incomplete annealing of the primer to the template. The fraction of annealed primer was determined by gel shift experiments and/or by prolonged incubation with excess RT and dNTPs. Wild-type HIV-1 RT and RNase H(–) HIV-1 RT bearing the E478Q point mutation were purified essentially as described (Le Grice and Grueninger-Leitch, 1990). Unless otherwise stated, the RNase H(–) RT was used in order to prevent cleavage of the RNA template when using the ODN. We showed previously that both RTs are equally efficient in initiating reverse transcription (Isel *et al.*, 1996).

Kinetic experiments

In steady-state experiments, excess primer–template was pre-incubated with HIV-1 RT for 4 min at 37°C in 50 mM Tris–HCl pH 8.0, 50 mM

KCl, 6 mM $MgCl_2$ and 1 mM dithioerythritol. Reverse transcription was initiated by adding either dCTP or dCTP plus dTTP at a final concentration of 50 μM. The reaction was stopped at increasing intervals by adding formamide containing 50 mM EDTA to aliquots of the reaction mixture.

The principle of the single turnover kinetics was the same except that RT was in excess compared with the primer–template. When $tRNA_3^{Lys}$ or $utRNA_3^{Lys}$ were the primers, reaction was slow and required no special equipment. For data points ranging from 1 to 6 s, drops of reagents were placed on a parafilm sheet and we worked in a room thermostatted at 37°C. Reactions were started and stopped by rapid mixing of the drops. The mixing time was estimated to be <0.5 s. For longer reaction times, the reagents were incubated in Eppendorf tubes in a water bath. The ODN-primed reaction was fast and required a quenched-flow apparatus. We used a home-built apparatus that allows determination of a complete reaction curve in one stroke (Gangloff *et al.*, 1984). This apparatus allows reaction times ranging from 5 to 450 ms. In this case, the reaction was stopped by addition of EDTA and sodium acetate at 25 mM and 750 mM final concentrations, respectively. Samples were precipitated and redissolved in formamide before analysis on sequencing gels.

Equilibrium binding constant and dissociation rate of primer–template–RT complex

In order to determine the binding constant of HIV-1 RT to the primer–template complexes, increasing concentrations of RT and primer–template [at a constant RT:(primer–template) ratio] were pre-incubated as described above. The ternary complexes were then extended by addition of dCTP and dTTP together with poly(rA)·$(dT)_{15}$ at a final concentration of 1 μM of $(dT)_{15}$, and the reaction was stopped after 30 s by addition of EDTA and formamide. Prior to addition in the reaction mixture, poly(rA) and $(dT)_{15}$ at a 10:1 ratio (w/w) were annealed at 70°C for 20 min. The efficiency of poly(rA)·$(dT)_{15}$ to trap free RT was controlled by checking that primer extension did not significantly increase from 15 s to 15 min.

In order to measure dissociation of RT from the ternary complex, the primer–template–RT complex was pre-formed as described above. After 4 min, 1 μM poly(rA)·$(dT)_{15}$ was added to trap RT that dissociated from the complex and aliquots were removed at several time intervals after addition of the trap, and mixed with dCTP and dTTP to extend the remaining ternary complex. Extensions were stopped after 30 s with EDTA and formamide.

Data analysis

For all experiments, the reaction products were analysed on 15% (ODN primer) or 8% ($tRNA_3^{Lys}$ and $utRNA_3^{Lys}$ primers) denaturing polyacrylamide gels and quantified with a BioImager BAS 2000 (Fuji) using the whole band analyser software (Bio Image). Curve fitting was performed with the SigmaPlot (Jandel) software.

Acknowledgements

We thank G.Keith and M.Yussupov for their help in the purification of $tRNA_3^{Lys}$, and J.Gangloff for technical advice concerning the quenched-flow apparatus. Thanks are also due to P.Bénas, P.Dumas, C.Isel, M.Yussupov and G.Yussupova for fruitful discussions. This work was supported by the French Agence Nationale de Recherches sur le SIDA (ANRS). S.Le G. is supported by grant AI31147 from the National Institutes of Health.

References

Aiyar,A., Cobrinik,D., Ge,Z., Kung,H.J. and Leis,J. (1992) Interaction between retroviral U5 RNA and the TψC loop of the $tRNA^{Trp}$ primer is required for efficient initiation of reverse transcription. *J. Virol.*, **66**, 2464–2472.

Aiyar,A., Ge,Z. and Leis,J. (1994) A specific orientation of RNA secondary structure is required for initiation of reverse transcription. *J. Virol.*, **68**, 611–618.

Arnold,E. *et al.* (1992) Structure of HIV-1 reverse transcriptase DNA complex at 7-Å resolution showing active site locations. *Nature*, **357**, 85–89.

Baltimore,D. (1970) Viral RNA-dependent DNA polymerase. *Nature*, **226**, 1209–1211.

Beard,W.A. and Wilson,S.H. (1993) Kinetic analysis of template–primer interactions with recombinant forms of HIV-1 reverse transcriptase. *Biochemistry*, **32**, 9745–9753.

DeStefano,J.J., Bambara,R.A. and Fay,P.J. (1993) Parameters that influence the binding of human immunodeficiency virus reverse transcriptase to nucleic acid structures. *Biochemistry*, **32**, 6908–6915.

Friant,S., Heyman,T., Wilhelm,M.L. and Wilhelm,F.X. (1996) Extended interactions between the primer $tRNA_i^{Met}$ and genomic RNA of the yeast Ty1 retrotransposon. *Nucleic Acids Res.*, **24**, 441–449.

Gangloff,J., Pouyet,J., Kern,D. and Dirheimer,G. (1984) A quenched-flow apparatus which allows the measurement of the kinetics of a reaction in one stroke. *J. Biochem. Biophys. Methods*, **9**, 201–213.

Gilboa,E., Mitra,S.W., Goff,S. and Baltimore,D. (1979) A detailed model of reverse transcription and tests of crucial aspects. *Cell*, **18**, 93–100.

Hsieh,J.C., Zinnen,S. and Modrich,P. (1993) Kinetic mechanism of the DNA-dependent DNA polymerase activity of human immunodeficiency virus reverse transcriptase. *J. Biol. Chem.*, **268**, 24607–24613.

Isel,C., Marquet,R., Keith,G., Ehresmann,C. and Ehresmann,B. (1993) Modified nucleotides of $tRNA_3^{Lys}$ modulate primer/template loop–loop interaction in the initiation complex of HIV-1 reverse transcription. *J. Biol. Chem.* **268**, 25269–25272.

Isel,C., Ehresmann,C., Keith,G., Ehresmann,B. and Marquet,R. (1995) Initiation of reverse transcription of HIV-1: secondary structure of the HIV-1 RNA/$tRNA_3^{Lys}$ (template/primer) complex. *J. Mol. Biol.*, **247**, 236–250.

Isel,C., Lanchy,J.M., Le Grice,S.F.J., Ehresmann,C., Ehresmann,B. and Marquet,R. (1996) Specific initiation and switch to elongation of human immunodeficiency virus type 1 reverse transcription require the post-transcriptional modifications of primer $tRNA_3^{Lys}$. *EMBO J.*, **15**, 917–924.

Jacobo-Molina,A. *et al.* (1993) Crystal structure of human immunodeficiency virus type-1 reverse transcriptase complexed with double-stranded DNA at 3.0 angstrom resolution shows bent DNA. *Proc. Natl Acad. Sci. USA*, **90**, 6320–6324.

Jaju,M., Beard,W.A. and Wilson,S.H. (1995) Human immunodeficiency virus type 1 reverse transcriptase—3′-azidodeoxythymidine 5′-triphosphate inhibition indicates two-step binding for template-primer. *J. Biol. Chem.*, **270**, 9740–9747.

Kati,W.M., Johnson,K.A., Jerva,L.F. and Anderson,K.S. (1992) Mechanism and fidelity of HIV reverse transcriptase. *J. Biol. Chem.*, **267**, 25988–25997.

Kohlstaedt,L.A., Wang,J., Friedman,J.M., Rice,P.A. and Steitz,T.A. (1992) Crystal structure at 3,5 Å resolution of HIV-1 reverse transcriptase complexed with an inhibitor. *Science*, **256**, 1783–1790.

Le Grice,S.F.J. and Grueninger-Leitch,F. (1990) Rapid purification of homodimer and heterodimer HIV-1 reverse transcriptase by metal chelate affinity chromatography. *Eur. J. Biochem.*, **187**, 307–314.

Marquet,R., Baudin,F., Gabus,C., Darlix,J.L., Mougel,M., Ehresmann,C. and Ehresmann,B. (1991) Dimerization of human immunodeficiency virus (type 1) RNA: stimulation by cations and possible mechanism. *Nucleic Acids Res.*, **19**, 2349–2357.

Marquet,R., Isel,C., Ehresmann,C. and Ehresmann,B. (1995) tRNAs as primer of reverse transcriptase. *Biochimie*, **77**, 113–124.

Martin,C.T., Muller,D.K. and Coleman,J.E. (1988) Processivity in early stages of transcription by T7 RNA polymerase. *Biochemistry*, **27**, 3966–3974.

McClure,W.R. (1985) Mechanism and control of transcription initiation in prokaryotes. *Annu. Rev. Biochem.*, **54**, 171–204.

Patel,H.P., Jacobo-Molina,A., Ding,J., Tantillo,C., Clark,A.D.J., Raag,R., Nanni,R.G., Hughes,S.H. and Arnold,E. (1995) Insights into DNA polymerization mechanisms from structure and function analysis of HIV-1 reverse transcriptase. *Biochemistry*, **34**, 5351–5363.

Patel,S.S., Wong,I. and Johnson,K.A. (1991) Pre-steady-state kinetic analysis of processive DNA replication including complete characterization of an exonuclease-deficient mutant. *Biochemistry*, **30**, 511–525.

Reardon,J.E. (1992) Human immunodeficiency virus reverse transcriptase—steady-state and pre-steady-state kinetics of nucleotide incorporation. *Biochemistry*, **31**, 4473–4479.

Reardon,J.E. (1993) Human immunodeficiency virus reverse transcriptase—a kinetic analysis of RNA-dependent and DNA-dependent DNA polymerization. *J. Biol. Chem.*, **268**, 8743–8751.

Rittinger,K., Divita,G. and Goody,R.S. (1995) Human immunodeficiency virus reverse transcriptase substrate-induced conformational changes and the mechanism of inhibition by nonnucleoside inhibitors. *Proc. Natl Acad. Sci. USA*, **92**, 8046–8049.

Shimamoto,T., Hsu,M.Y., Inouye,S. and Inouye,M. (1993) Reverse transcriptases from bacterial retrons require specific secondary structures at the 5′-end of the template for the cDNA priming reaction. *J. Biol. Chem.*, **268**, 2684–2692.

Spence,R.A., Kati,W.M., Anderson,K.S. and Johnson,K.A. (1995) Mechanism of inhibition of HIV-1 reverse transcriptase by nonnucleoside inhibitors. *Science*, **267**, 988–993.

Temin,H.M. and Mizutani,S. (1970) RNA-dependent DNA polymerase in virions of rous sarcoma virus. *Nature*, **226**, 1211–1213.

von Hippel,P.H., Bear,D.G., Morgan,W.D. and McSwiggen,J.A. (1984) Protein–nucleic acid interactions in transcription: a molecular analysis. *Annu. Rev. Biochem.*, **53**, 389–446.

Wakefield,J.K., Kang,S.-M. and Morrow,C.D. (1996) Construction of a type 1 human immunodeficiency virus that maintains a primer binding site complementary to $tRNA^{His}$. *J. Virol.*, **70**, 966–975.

Wang,H. and Lambowitz,A.M. (1993) The mauriceville plasmid reverse transcriptase can initiate cDNA synthesis de novo and may be related to reverse transcriptase and DNA polymerase progenitor. *Cell*, **75**, 1071–1081.

Wang,G.H. and Seeger,C. (1992) The reverse transcriptase of hepatitis-B virus acts as a protein primer for viral DNA synthesis. *Cell*, **71**, 663–670.

Wilhelm,M., Wilhelm,F.X., Keith,G., Agoutin,B. and Heyman,T. (1994) Yeast ty1 retrotransposon: the minus-strand primer binding site and a cis-acting domain of the ty1 RNA are both important for packaging of primer tRNA inside virus-like particles. *Nucleic Acids Res.*, **22**, 4560–4565.

Wong,I., Patel,S.S. and Johnson,K.A. (1981) An induced-fit kinetic mechanism for DNA replication fidelity: direct measurement by single-turnover kinetics. *Biochemistry*, **30**, 526–537.

Zimmerly,S., Guo,H.T., Perlman,P.S. and Lambowitz,A.M. (1995) Group II intron mobility occurs by target DNA-primed reverse transcription. *Cell*, **82**, 545–554.

Received on June 3, 1996; revised on August 27, 1996